First-order phase transition in a three-dimensional vortex system: Modeling $Bi_2Sr_2CaCu_2O_8$ in high magnetic fields

Leonardo P. Viana,* E. P. Raposo,† and M. D. Coutinho-Filho‡
Laboratório de Física Teórica e Computacional, Departamento de Física, Universidade Federal de Pernambuco, Recife, PE 50670-901, Brazil

(Received 16 September 2003; revised manuscript received 14 June 2004; published 26 October 2004)

The nature of the vortex matter and its phase transitions in high-temperature superconducting oxides still present open issues, although results from a number of experiments and theoretical studies do support first-order transitions both at low and high applied magnetic fields. We report on first-order melting transitions obtained via Monte Carlo simulations using the Lawrence-Doniach (LD) model for vortices in strongly anisotropic layered superconductors, focusing on a clean three-dimensional sample of $Bi_2Sr_2CaCu_2O_8$, with dc magnetic field perpendicular to the CuO_2 superconducting planes. In particular, our investigations indicate that in the high-field regime the CuO_2 planes decouple at the melting transition, in agreement with very recent experimental observations. Moreover, contrary to some theoretical suggestions, we confirm Nelson's predictions for the random-walk-like diffusion of the melted lines along the direction of the applied field. Our results extend and clarify previous studies using the LD model and suggest the reliability of this framework in describing strongly anisotropic layered superconductors.

DOI: 10.1103/PhysRevB.70.134516 PACS number(s): 74.25.Dw, 74.25.Qt, 74.72.Hs

I. INTRODUCTION

Despite the great progress achieved along the years, the (H,T) phase diagram of high-temperature (high-T_c) superconductors is still not completely established. In fact, recently there has been a revival concerning the true nature of the vortex matter and its transitions in anisotropic materials, such as $Bi_2Sr_2CaCu_2O_8$ (BSCCO) (Refs. 1–4) and $YBaCu_3O_7$ (YBCO) (Ref. 5) compounds. Particularly in BSCCO, the nature of the transition lines in intermediate and high fields, $B > B_{cr} \sim 0.1$ T (see discussion below), such as the depinning, melting, and decoupling lines, is still a matter of controversy.[1,3,4,6,7] Furthermore, even with conventional superconductors, like pure niobium, the vortex matter transition is still matter of discussion[8] on whether an experimentally observed transition is associated to the melting[9] or to the disordering of the flux lines due to the enhancement of the flux line pinning in the peak effect region.[10,11]

On the theoretical side, Nelson and Seung[12] have presented the well-known mapping of the three-dimensional (3D) vortex system onto the 2D nonrelativistic interacting boson system and, using Lindemann-like criteria,[13,14] predicted the behavior of several lines in the (H,T) phase diagram. Some of Nelson's[12] results concerning line entanglement have been questioned[15] with the suggestion that, at least in the low-density limit of the flux-line liquid, the vortex system might be in a "weakly" entangled state, where the average width of the flux lines can be much larger than the average intervortex distance, but does not diverge with sample thickness, in contradiction to Nelson's "fully" entangled liquid phase. Moreover, Nguyen and Sudbø[16] have imposed some restrictions to the regime of validity of Nelson's scenario, which in fact has already been extended to include nonlocal elastic effects.[17,18] Through a Monte Carlo (MC) simulation of the uniformly frustrated 3D *XY* model,[19–22] these authors[16] have identified a second transition associated with the unbinding of vortex-loop thermal excitations at temperatures above the melting line. In this regime the lines-only approximation does not provide a suitable description of the system. Previous theoretical studies on the vortex phase diagram of *clean* anisotropic high-T_c superconductors also include simulations using the lattice London,[23] lowest-Landau level,[24,25,28] 2D-boson path-integral,[26] and the Lawrence-Doniach[27,29,30] models. In closing this discussion, we should remark that, in spite of more than a decade of theoretical, numerical, and experimental studies, the question of whether vortices can form an entangled state has not yet been convincingly answered.[7]

Our main concern in this work is to investigate the suitability of the Lawrence-Doniach-Ginzburg-Landau model,[27] or simply the Lawrence-Doniach (LD) model, of stacked superconducting planes in describing vortex matter in highly anisotropic layered superconductors, such as BSCCO compounds. We report on first-order melting transitions in intermediate and high magnetic fields obtained by detailed numerical MC simulations using the LD model, focusing on a clean 3D sample of BSCCO with applied dc magnetic field H along the z axis perpendicular to the CuO_2 superconducting *ab* planes. Despite the importance of disorder in the vortex phase diagram, as can be appreciated in a recent observation of a Bragg glass phase in BSCCO and other high- T_c materials,[31] these effects are not included in our results, since, as emphasized by Nelson[32] and Nelson and Le Doussal,[33] weak point disorder affects the (H,T) phase diagram only for quite low magnetic fields (see, e.g., Fig. 2 in Ref. 30).

Our investigations on the melting transition extend previous results on the same model[27,29,30,34] and further characterize the role of line entanglement and decoupling in the phase diagram of the 3D vortex system. The occurrence of the first-order melting transition is determined by the presence of discontinuity in the amplitude of the first Bragg peak of the

planar density-density correlation function, in the rms deviation of the mean planar position of the vortices, in the hexatic order parameter, and in the mean planar distance between vortices. No evidence of an hexatic phase between the solid and liquid ones has been found, despite early expectations[35] and LD simulation results.[27] Our results on the end-to-end displacement of the flux lines have confirmed Nelson and Seung's predictions[12] for the random-walk-like diffusion along the applied field direction of melted lines, in agreement with *XY* MC results,[19,20] as well as with the "cage" confinement of the flux lines in the solid phase.[12] In addition, our numerical data on the *z*-dependent density-density correlation function indicate that in the high-field regime the flux lattice melts into a decoupled liquid of pancake vortices, in agreement with recent experimental observations in BSCCO,[1] but in disagreement with previous LD simulation results.[29]

This paper is organized as follows: in Sec. II we review the line modeling of vortex matter in BSCCO, focusing on the analogy of 2D-interacting bosons and 3D interacting vortex lines and on the LD line model to describe vortex lines in layered superconductors; Sec. III is devoted to the presentation and discussion of our simulation results on the light of previous model predictions, simulations, and recent experimental results; finally, in Sec. IV we present our concluding remarks.

II. LINE MODELING OF VORTEX MATTER IN BSCCO

A. Boson mapping, entanglement, and decoupling

The study of the vortex properties in high-temperature superconductors has become a topical subject in statistical mechanics and condensed-matter physics.[13,35,36] This is mainly due to the strong effects of thermal fluctuations and anisotropy in the vortex lattice of such materials, giving rise to a large region of vortex liquid phase in the (H,T) phase diagram, contrasting with conventional type-II superconductors in which the flux lines form a lattice up to the upper critical field H_{c_2}.[20]

Nelson[12] has observed the analogy between the Gibbs free energy of 3D interacting vortex lines in a highly anisotropic superconductor with H parallel to the symmetry axis z, and the imaginary time action of 2D interacting bosons world "lines" at finite T. In this mapping, the imaginary time ruled by T in the 2D boson system is equivalent to the third dimension z in the 3D vortex system. Under this analogy, a random-walk picture of the transverse motion of a flux line as it meanders along the z axis leads to the conclusion that the vortex line *diffuses* as a function of the timelike variable z:

$$\Delta r_z \equiv \sqrt{\langle [\mathbf{r}_i(z) - \mathbf{r}_i(0)]^2 \rangle} = \sqrt{2Dz}, \tag{1}$$

where $\mathbf{r}_i(z)$ is the position of the line i in the plane z, $\langle \cdots \rangle$ represents thermal average, and $D=(M/m)[4\pi k_B T/(\phi_0 H_{c_1})]$ is the diffusion constant,[12] with M/m denoting the uniaxial anisotropy, k_B the Boltzmann constant, ϕ_0 the quantum of magnetic flux, and H_{c_1} the lower critical field. Further, an entanglement correlation length is defined as the average spacing between collisions in a vortex liquid with areal density $n=B/\phi_0$:[37]

$$\xi_{z,c} \equiv \frac{1}{8nD} = \frac{\tilde{\epsilon}}{8k_B T n}, \tag{2}$$

in which B is the magnetic induction and $\tilde{\epsilon} \equiv k_B T/D$. The collisions and entanglement of the flux lines then determine the characteristics of the vortex system whenever $L_z \gg \xi_{z,c}$, where L_z is the sample thickness.

The phase diagram of the 2D-interacting boson system has three distinct phases: crystal, normal liquid, and superfluid, which correspond in the clean 3D vortex system to the Abrikosov lattice, disentangled liquid, and entangled liquid of lines, respectively.[26] As L_z increases in the superconducting sample (or, equivalently, as T decreases in the boson system), the disentangled liquid phase (normal liquid of 2D bosons) becomes not accessible. Indeed, for sufficiently thick samples the average radial distance between the ends of the vortex line, Δr_{L_z}, is larger than the average distance between two neighbor lines, $a_0 \equiv (\sqrt{2/\sqrt{3}})\sqrt{\phi_0/B}$, therefore implying that, once the vortex lattice of such thick samples melts, it forms a liquid of entangled lines with continuous translational symmetry in the planes. Thus the criterion

$$\Delta r_{L_z} \geqslant a_0/2, \tag{3}$$

assigned for the entangled liquid phase, assumes that its onset occurs when the projection of each line onto the *ab* plane touches the projection of its neighbors. In such a case, the vortex lines lose their individuality. On the other hand, for thinner samples, a phase of disentangled line liquid might emerge, in which

$$\Delta r_{L_z} < a_0/2. \tag{4}$$

In a layered anisotropic superconductor, by a similar criterion, adjacent layers may decouple and the vortex system would become a pile of weakly coupled 2D "pancake" vortices in the *ab* planes, with the average distance between pancakes of the same flux line in adjacent planes,

$$\Delta r_1 \equiv \sqrt{\langle [\mathbf{r}_i(z+1) - \mathbf{r}_i(z)]^2 \rangle}, \tag{5}$$

satisfying

$$\Delta r_1 \geqslant a_0/2. \tag{6}$$

In this case, although the line model is no longer strictly adequate to describe the vortices, it seems that the random-walk picture may still provide a suitable description of the liquid phase, at least close to the melting transition.

B. Lawrence-Doniach line model

Besides the two length scales usually associated with superconducting properties, namely the planar correlation length ξ_{ab} and the planar penetration depth λ_{ab}, while dealing with vortex matter it is convenient to introduce a B-dependent scale: $a_0(\propto B^{-1/2})$, the mean distance between nearest-neighboring vortices. Moreover, in anisotropic superconductors one also considers an additional anisotropy-

related length scale γd, where $\gamma=\lambda_z/\lambda_{ab}$ measures the ratio between axial and planar penetration depths, and d is the distance between adjacent ab planes. Such scale marks the onset above which the Josephson interaction between pancake vortices in adjacent layers can no longer be considered approximately quadratic [see Eq. (14) below].

Whenever the scales involved in vortex matter are such that $\xi_{ab} \ll a_0 \ll \lambda_{ab}$ and $\lambda_{ab} \gg \gamma d$, the magnetic induction B in the superconducting sample is essentially constant. This scenario favors descriptions through XY models, which consider only phase variations in the superconducting order parameter,[16,20,21] and are expected to hold for YBCO and anisotropically similar compounds ($\gamma \lesssim 20$). In contrast, in much stronger anisotropic compounds ($\gamma \gtrsim 50$), such as BSCCO, the scales are such that[21] $\lambda_{ab} \sim \gamma d$. Under these conditions, nonuniformities of the magnetic induction become relevant, making 3D frustrated XY models less adequate, while the LD model may appear as a more realistic description.

The starting point of our simulations is the Lawrence-Doniach-Ginzburg-Landau model of stacked superconducting planes.[27,38] The LD free energy is given by

$$F_{LD} = \frac{1}{8}\int d^3r\, \mathbf{B}^2(r) + \frac{dH_c^2(0)}{8\pi}\sum_{z=1}^{L_z}\int d^2\rho \Bigg\{ \left(1-\frac{T}{T_c}\right)|\psi_z|^2 + \frac{1}{2}\beta|\psi_z|^4 + |\xi_{ab}(T)(\nabla_{ab} - i2e\mathbf{A}_{ab})\psi_z|^2 - g\left|\exp\left(2ie\int_{z_{n+1}}^{z_n} dz\, A_z \psi_{z+1} - \psi_z\right)\right|^2 \Bigg\}, \quad (7)$$

where ψ_z denotes the superconducting order parameter, g is the interlayer Josephson coupling strength, $H_c(T)$ the thermodynamic critical field, e the charge of the electron, β the Landau coefficient of the quartic term in $|\psi_z|$, ∇_{ab} the in-plane gradient, $\mathbf{A}_{ab}$ the vector potential in the ab plane, and T_c the zero-field critical temperature. The above Helmholtz free energy is considered instead of the Gibbs one: $G=F-(1/4\pi)\int d^3r\, \mathbf{B}\cdot\mathbf{H}$, since in our simulations we consider fixed B (constant number of vortices) along the z axis of the sample. Moreover, for a single flux line crossing two adjacent CuO_2 planes, the Josephson coupling among line segments at the two planes can be shown to be larger than the magnetic interaction between them by a factor $\sim g(\lambda_{ab}/\xi_{ab})^2(d/s)^2 \sim 10$ for BSCCO,[27,39] where s is the layer thickness. Indeed, the electromagnetic interaction between layers has been shown to be relevant only in the low-field part of the phase diagram, $B<0.1$ T for BSCCO parameters,[40] and therefore it is not considered here. Also, the interaction of a flux line with the external magnetic field can be shown to be negligible.[27] At last, B-independent pinning disorder is also not included since in the high-field regime it is overwhelmed by the in-plane magnetic interaction between vortices.

From the above considerations, we assume[27] that the LD free energy is dominated by two energy scales, namely the Josephson energy density ϵ_J, which accounts for the interaction between pancake vortices of a single flux line in adjacent layers, and the magnetic repulsion energy density ϵ_m, which stands for the repulsion between segments of distinct flux lines in the same plane. These two densities are connected with the anisotropy and material parameters by the relations

$$\epsilon_J \equiv \frac{dE_J}{dV} = \frac{1}{2}\frac{H_c^2(0)}{8\pi}g, \quad (8)$$

$$\epsilon_m \equiv \frac{dE_m}{dV} = \frac{H_c^2(0)}{8\pi}\frac{\xi_{ab}^2(0)}{l_{ab}^2(B)} = \frac{1}{l_{ab}^2(B)}\left(\frac{\phi_0^2}{64\pi^3\lambda_{ab}^2(0)}\right), \quad (9)$$

where $l_{ab}(B)$ defines a length scale in the ab plane, such that

$$\frac{\epsilon_m}{\epsilon_J} = \frac{2\xi_{ab}^2(0)}{g l_{ab}^2(B)}. \quad (10)$$

Whenever the two energy scales become comparable, one finds

$$l_{ab,cr} = \frac{\sqrt{2}\xi_{ab}(0)}{\sqrt{g}}, \quad (11)$$

which defines the critical field

$$B_{cr} = \frac{\phi_0}{l_{ab,cr}^2} = \frac{\phi_0 g}{2\xi_{ab}^2(0)}, \quad (12)$$

above which the system behaves as a vortex lattice with weakly interacting adjacent planes. Since $\gamma = l_{ab,cr}/d = \sqrt{2}\xi_{ab}(0)/(\sqrt{g}d)$, then, using BSCCO parameters $\gamma \simeq 100$, $\xi_{ab}(0)=21$ Å, and $d=15$ Å, one finds $1/\sqrt{g}=50$ and $B_{cr} \simeq 900$ G.

Our simulations are thus performed for $B > B_{cr}$ within the framework introduced by Ryu and co-workers,[27] based on the LD model, in which the repulsion magnetic energy between pancake vortices in the same plane is given by

$$\frac{\phi_0^2 s}{8\pi^2\lambda_{ab}^2} K_0\left(\frac{|\mathbf{r}_{ij}(z)|}{\lambda_{ab}}\right), \quad (13)$$

where $\mathbf{r}_{ij}(z) \equiv \mathbf{r}_j(z) - \mathbf{r}_i(z)$, K_0 represents the modified Bessel function of order zero, and $\lambda_{ab}(T) = \lambda_0(1-T/T_c)^{-1/2}$ denotes the planar penetration length at a temperature T, with $\lambda_0 \equiv \lambda_{ab}(T=0)$. In addition, the Josephson coupling between pancake vortices belonging to the same flux line in adjacent layers reads[27]

$$\frac{d\phi_0^2}{8\pi^3\lambda_{ab}^2}\left[1+\ln\left(\frac{\lambda_{ab}}{d}\right)\right]\left(\frac{r_1^2}{(\gamma d)^2}-1\right), \quad \text{for} \quad r_1 \leqslant \gamma d,$$

$$\frac{d\phi_0^2}{4\pi^3\lambda_{ab}^2}\left[1+\ln\left(\frac{\lambda_{ab}}{d}\right)\right]\left(\frac{r_1}{\gamma d}-1\right), \quad \text{for} \quad r_1 > \gamma d, \quad (14)$$

in which $r_1 \equiv |\mathbf{r}_i(z+1) - \mathbf{r}_i(z)|$. Although for very high fields,[20,41] $B \gg B_{cr}$, the Josephson coupling needs a nonpairwise and nonlocal treatment, we take the pairwise interaction, as in Eq. (14), particularly to allow the computation feasibility of this 3D model system in the range of parameters used to study the (B,T) phase diagram. In this sense, since the potential energy between pancakes in neighbor lay-

ers is still attractive for large $B(a_0 \gtrsim \gamma d)$, Eq. (14) essentially introduces an effective spring constant associated to small displacements from equilibrium.[27] On the other hand, for larger displacements we assume that an interplanar core will start to form with energy proportional to the distance between the pancakes.

III. SIMULATION RESULTS

In our MC simulations we have considered a system of 64 flux lines confined to a grid of $256 \times 222 \times L_z$, with $L_z = 64$ layers and periodic boundary conditions in all directions. Each flux line may be viewed as a collection of beads (pancake vortices) connected by a flexible string along the z axis, with each bead restricted to move in an ab plane. The grid lattice in the planes is triangular in order to be commensurable with the Abrikosov lattice. In a single MC step (MCS) every bead makes a trial movement by a unit grid through the Metropolis algorithm. We start with the triangular Abrikosov lattice at $T = 1$ K and then slowly increase T by small steps ΔT, discarding the first n_0 MCS for equilibration in the averaging process. We perform simulations using: (i) 10^5 MCS, $n_0 = 2 \times 10^4$ MCS, and $\Delta T = 0.2$ K; and (ii) 10^6 MCS, $n_0 = 2 \times 10^5$ MCS, and $\Delta T = 1$ K ($\Delta T = 0.2$ K near the melting transition). These choices for the MC running times, n_0 and ΔT, were made in order to assure convergence of the MC results with regard to the system size and region of the phase diagram. Indeed, some of our preliminary test studies using, for instance, only 2×10^4 MCS led to strongly time-dependent results, mainly inthe vicinity of the melting transition, including some spurious numerical effects in the low-field regime. Furthermore, we have chosen the following parameters suitable to describe a BSCCO sample:[13] $d = 15$ Å, $s = 1.66$ Å, $\lambda_0 = 1414.2$ Å, $T_c = 87$ K, and the ones listed below Eq. (12) of the previous section.

The two symmetries present in the vortex line model, namely the in-plane symmetry and the one along the z axis, pose the question of whether they can be broken separately or simultaneously.[23] In the former case, the possibility of a supersolid (broken translational symmetry only) or a disentangled liquid (broken z-axis symmetry only) phase arises. Otherwise, the simultaneous symmetry breaking leads to an entangled or even decoupled liquid state. In our simulations in the high-field regime, we have observed discontinuity at the melting temperature $T_m(B)$, in several quantities related to both planar and longitudinal symmetries, thus revealing the first-order character of this transition. For instance, as T increases, Fig. 1 displays, for $B \geqslant 1$ T, the sudden disappearance at $T = T_m$ of the first Bragg peak of the structure factor in the momentum $\mathbf{k} = (k_x, k_y)$ space, $S(\mathbf{k}_{Bragg})$, with $S(\mathbf{k}) \equiv S(\mathbf{k}, z = 0)$, and

$$S(\mathbf{k}, z) = \frac{1}{\Omega N} \sum_{\mathbf{r}} \langle n(0,0) n(\mathbf{r}, z) \rangle e^{i\mathbf{k}\cdot\mathbf{r}}, \tag{15}$$

where $\langle n(0,0) n(\mathbf{r}, z) \rangle$ is the density-density correlation function in plane z, N is the number of lines, and Ω is the normalization factor [$S(\mathbf{k}_{Bragg}) = 1$ at $T = 1$ K]. In addition, the line-average in-plane rms displacement of a pancake vortex,

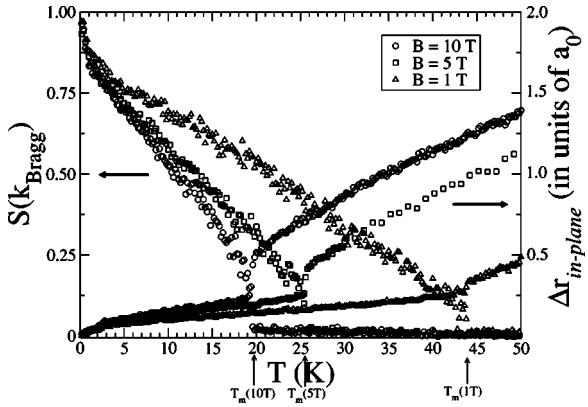

FIG. 1. T dependence of the planar structure factor at the first Bragg peak (left axis) and line-average in-plane rms displacement of pancake vortices (in units of a_0) (right axis) at fixed B. Vertical arrows locate the discontinuity in both observables, associated with the first-order melting line $T_m(B)$. Data using 10^5 MCS and $\Delta T = 0.2$ K.

$$\Delta r_{in\text{-}plane} \equiv \sqrt{\langle [\mathbf{r}_i(z) - \langle \mathbf{r}_i(z) \rangle]^2 \rangle}, \tag{16}$$

also suffers a discontinuity at $T_m(B)$ in the same field range, as shown in Fig. 1. At the onset of this discontinuity we notice that $\Delta r_{in\text{-}plane}/a_0 \simeq 0.2-0.3$, which corresponds to a Lindemann-like criterion. As a consequence, although this range of values of $\Delta r_{in\text{-}plane}/a_0$ at the melting line coincides with that reported in the literature,[21,27] a precise value of $T_m(B)$ should not be strictly determined from the Lindemann criterion, the most adequate one being that associated with a direct measure of the discontinuity in these observables at the melting transition.[16,20,30]

We should add that there exists a third symmetry associated with the in-plane orientational order. This may give rise to the possibility of an hexatic phase (with broken orientational symmetry only) between the liquid (with complete symmetry) and solid phases (with broken translational and orientational symmetries). In this context, we have measured the local orientational order parameter[35] (or hexatic order parameter[27,30]), defined as

$$\Psi_6 = \sum_{i=1}^{N} \frac{1}{z_i} \sum_{j=1}^{6} e^{6i\theta_{ij}}, \tag{17}$$

where z_i is the coordination number for the vortex i and θ_{ij} is the bond angle between neighbors i and j.

Our results displayed in Fig. 2(a) show that the hexatic order parameter vanishes at $T_m(B)$, along with the first Bragg peak of the structure factor, in agreement with previous numerical studies.[19–21,30] Indeed, even in a detailed simulation close to the melting transition [inset of Fig. 2(a)] we find no measurable hexatic phase, contrary to early results by Ryu *et al.*[27] using BSCCO parameters in a LD framework, but in agreement with more recent simulations by Ryu and Stroud[30] using YBCO parameters and the same model. Here it is worth mentioning that Nelson's description has predicted the existence of an hexatic phase[42] in high-T_c superconductors [for the melting of flux lines, see, e.g., Fig. 8.1(a) in Ref. 33].

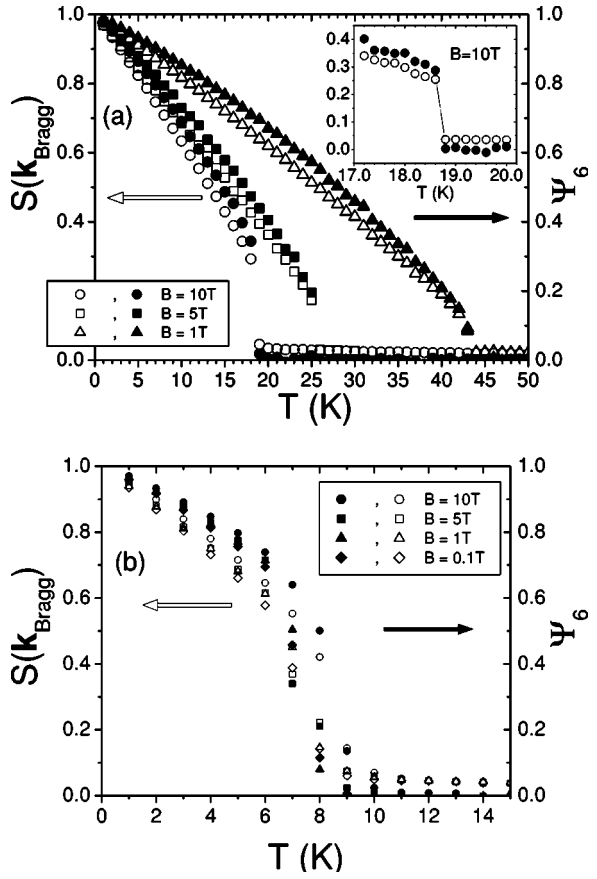

FIG. 2. T dependence of the planar structure factor at the first Bragg peak (open symbols; left axis) and the planar hexatic order parameter (filled symbols; right axis) at fixed B: (a) 3D LD model, with inset displaying a close view of the transition at $B=10$ T; (b) 2D (one layer) pancake vortex system. In both 2D and 3D cases observables vanish at the melting transition $T_m(B)$, thus showing no evidence of a hexatic phase. Data using 10^6 MCS and $\Delta T=1$ K [$\Delta T=0.2$ K in the inset of (a)].

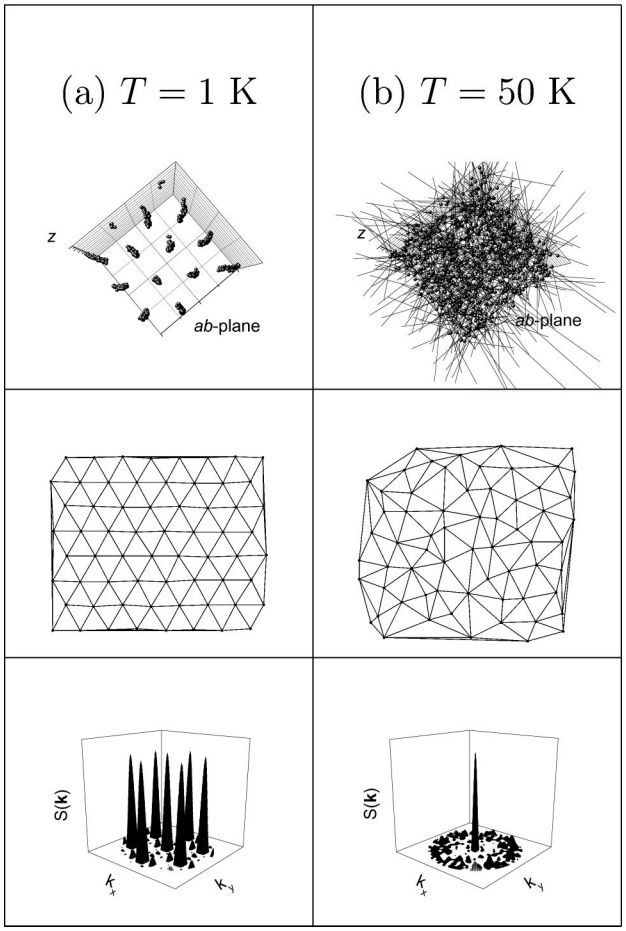

FIG. 3. From top to bottom: snapshots of part of the 3D vortex configuration from a top view, Delaunay triangulation of the 64 pancake vortices and its associated planar structure factor at fixed $B=10$ T. (a) At $T=1$ K vortices form an almost defect-free crystalline lattice with well defined first Bragg peaks; (b) at $T=50$ K $>T_m(B)$ the Bragg peaks have vanished in the fully symmetric liquid phase. Scales are the same for both temperatures. Data taken after 10^6 MC, using $\Delta T=1$ K.

Despite this fact, a number of simulation results[19–21,30] have agreed that the hexatic phase does not occur in high-T_c superconductors.

In addition, by closely observing Figs. 1 and 2(a) we notice that the discontinuity at $T_m(B)$ curve obtained using 10^6 MCS and $\Delta T=1$ K decreases by ≈ 1 K at $B=10$ T, as compared with the one using 10^5 MCS and $\Delta T=0.2$ K, although the data fluctuation in Fig. 1 is larger due to the smaller number of MC steps. In contrast, no significant difference was found in the $T_m(B)$ values at lower fields. We thus believe that in our simulation the vortex configurations have attained a regime of quasiequilibrium and that the observed first-order melting transition is a true thermodynamical one. Moreover, by performing a MC simulation of interacting pancakes in one single plane using 10^6 MCS and $\Delta T=1$ K, we obtain a field-independent (within numerical accuracy) temperature of dislocation-mediated 2D melting,[43] $T_m^{2D} \simeq 9$ K, see Fig. 2(b); as in the 3D vortex system, no evidence of an hexatic phase was found.

The above results, both in the configurational and momentum spaces, can be viewed through the evolution with T of the Delaunay triangulation of the vortex configurations in an ab plane and the magnitude of their associated $\mathbf{k}$-space planar structure factor $S(\mathbf{k})$. Figures 3 and 4 display the distinct patterns of the solid and liquid vortex phases at $B=10$ T. For $T \ll T_m(B)$ the pancake vortices present very low mobility and a pattern of regular peaks is clearly observed in the planar structure factor. As T approaches $T_m(B)$, the low-T crystalline Abrikosov lattice becomes more and more distorted by the presence of thermally induced defects, although the first Bragg peaks can still be distinguished. In such a case, though defects dominate the lattice, as shown by triangulation, the vortex configuration is still almost static, not freely switching to energetically similar ones. In contrast, slightly above $T_m(B)$, although the defect landscape looks similar to the one slightly below T_m (see Fig. 4), the mobility of the vortices increases considerably, thus allowing energetically similar configurations to be accessed. As a result, the first Bragg peaks collapse into an almost circular pattern, as typical of a fully symmetric liquid phase.

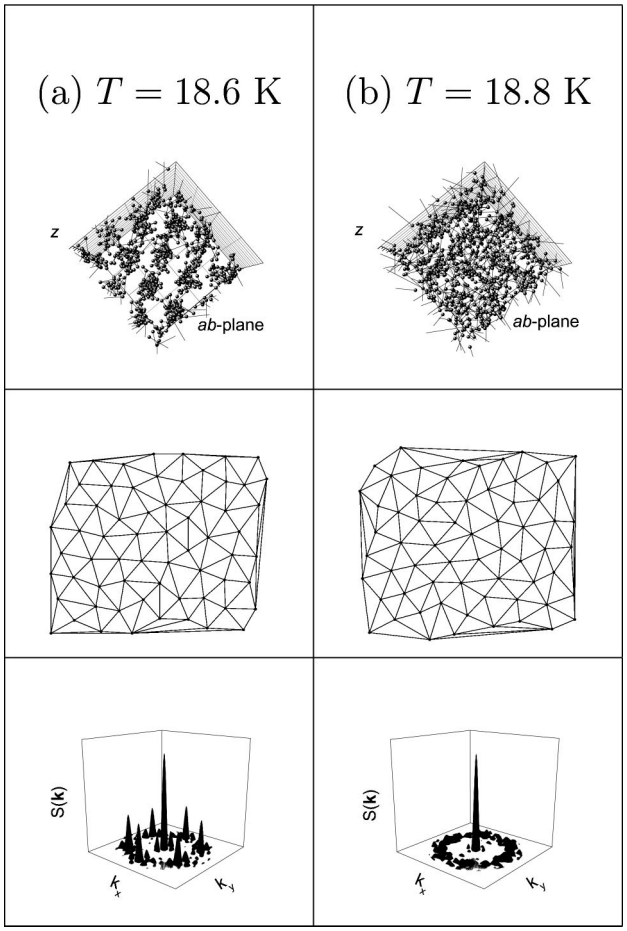

FIG. 4. Same as in Fig. 3 at fixed $B=10$ T and close to the melting transition, $T_m(B) \in$ (18.6 K, 18.8 K). Thesolid flux lattice is shown highly distorted slightly below the melting line [(a) $T=18.6$ K] and destructed just above it [(b) $T=18.8$ K]. Scales as in Fig. 3. Data taken after 10^6 MCS, using $\Delta T=0.2$ K.

In Fig. 5 we present data for the correlation length ξ_z along the applied field and close to the melting temperature, obtained by fitting the z-dependent decay of the structure factor, averaged over 14 configurations, with the expression[12]

$$S(\mathbf{k},z) = S(\mathbf{k},z=0)e^{-|z|/\xi_z}. \tag{18}$$

For high fields ($B=10$ and 5 T in Fig. 5) ξ_z changes abruptly at $T_m(B)$ from values larger than the half width of the sample (due to the periodic boundary condition in z) to values smaller or, at most, comparable to the distance between two adjacent layers, i.e., $\xi_z \lesssim d$. This indicates that in the high-field regime the flux lattice melts into a decoupled liquid of pancake vortices. This result contradicts those presented by Hellerqvist *et al.*,[29] in which measurements of the z-axis transport in a single BSCCO crystal for fields up to 9 T suggested that the decoupling of the superconducting CuO_2 layers occurs via a continuous crossover in this material, as also supplemented by MC simulations using the LD model.[29] Indeed, as shown in Fig. 4 of Ref. 27, the melting (irreversibility) and decoupling processes are clearly associated to distinct lines, as determined from experiments and MC LD simulations (e.g., these lines differ over 30 K for $H=2$ T). The discrepancies regarding our results may be attributed to the longer run times and larger samples used in our procedures.

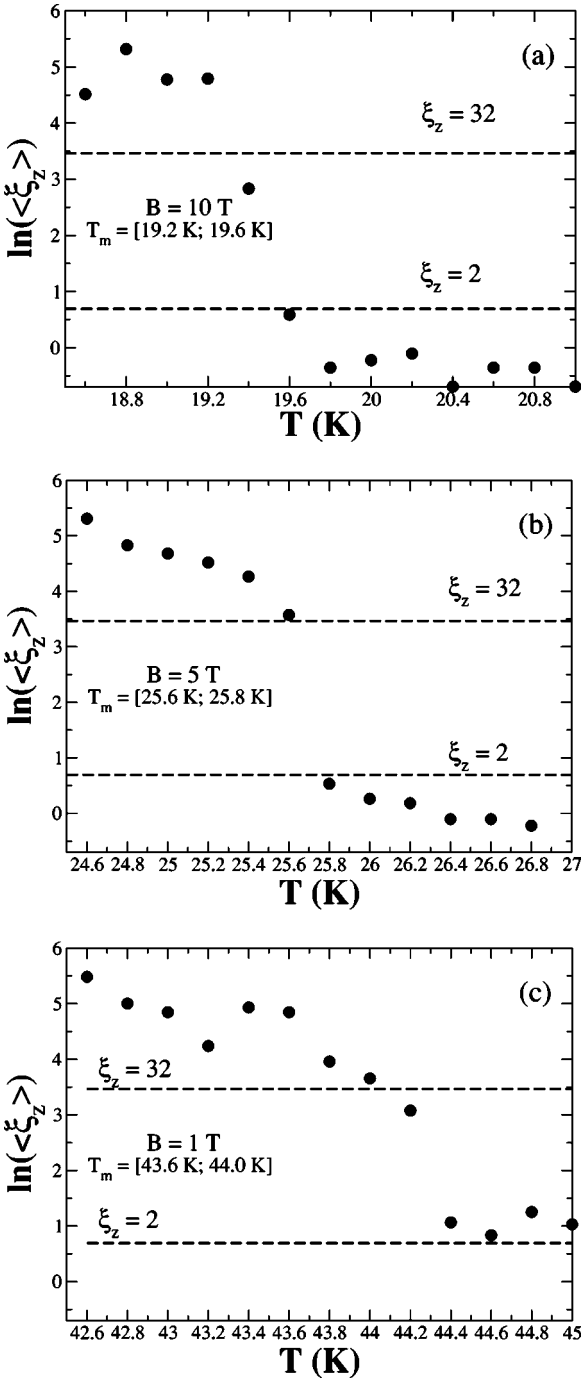

FIG. 5. T dependence of the correlation length (in units of d) along the applied field (z axis) at (a) $B=10$ T, (b) $B=5$ T, and (c) $B=1$ T, presenting discontinuity at the same temperature as $T_m(B)$ (see Figs. 1 and 2), above indicated by an interval. The upper and lower dashed lines correspond, respectively, to the half width $L_z/2(=32d)$ of the sample (due to the periodic boundary condition in z) and to $2d$. Data taken after 10^5 MCS, using $\Delta T=0.2$ K, and averaged over 14 samples.

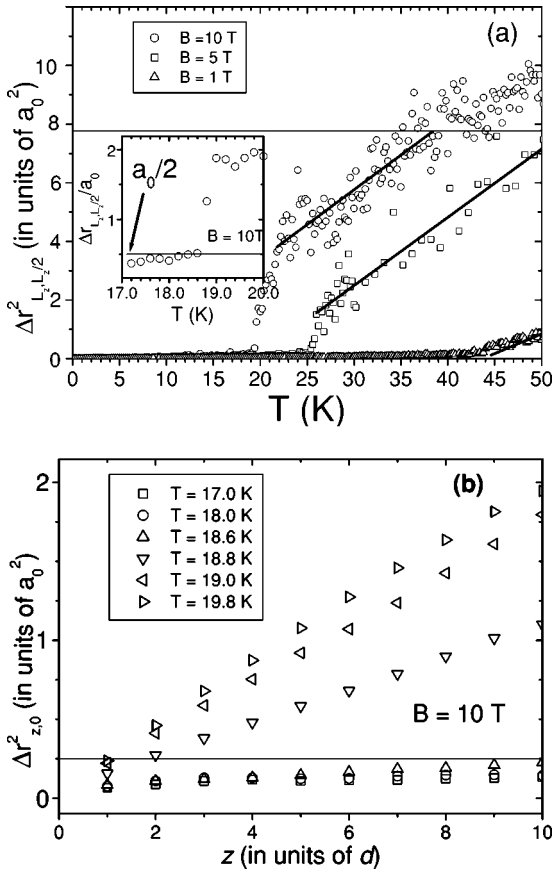

FIG. 6. (a) T dependence of the line-average end-to-end rms. displacement of vortex lines. For $B \geqslant 1$ T the discontinuity occurs at $T_m(B)$. Solid lines indicate best fittings to $\Delta r^2_{L_z,L_z/2} \propto T$. The horizontalline marks the onset of the regime in which finite size effects are expected to occur due to the periodic boundary conditions in the *ab* planes. Data using 10^5 MCS and $\Delta T = 0.2$ K. Inset: Details of the transition at $B = 10$ T; the horizontal line indicates the value $\Delta r_{L_z,L_z/2} = a_0/2$ usually associated to an entanglement criterion. Inset data using 10^6 MCS and $\Delta T = 0.2$ K. (b) The average displacements of the vortex lines in the z direction, at $B = 10$ T, and for temperatures below and above melting: $T_m(B) \in (18.6\text{ K}, 18.8\text{ K})$. Horizontal line, $\Delta r_{z,0} = a_0/2$, marks the saturation value of the average radial projection of a flux line in the vortex solid state. In the liquid phase, $\Delta r^2_{z,0} \propto z$; for larger values of z, saturation effects occur due to periodic boundary conditions. Data using 10^6 MCS and $\Delta T = 0.2$ K.

For lower fields ($B = 1$ T in Fig. 5), ξ_z above $T_m(B)$ is somewhat larger than d, thus indicating a possible crossover, as B decreases, to a liquid phase of entangled lines with weak axial correlation or the breaking of the system into an almost 2D pancake vortex liquid, i.e., $d \lesssim \xi_z \ll L_z$.

Figure 6 presents the rms displacement of the vortex lines in the z direction,

$$\Delta r_{z,z_0} \equiv \sqrt{\langle [r_i(z) - r_i(z_0)]^2 \rangle}. \tag{19}$$

As shown in Fig. 6(a), $\Delta r_{z,z_0}(T)$ also displays discontinuity at $T_m(B)$, where $z = L_z$ and $z_0 = L_z/2$ were taken due to the periodic boundary condition in z. Figure 6(b) shows the dependence on z of $\Delta r_{z,0}$ below and above the melting transition.

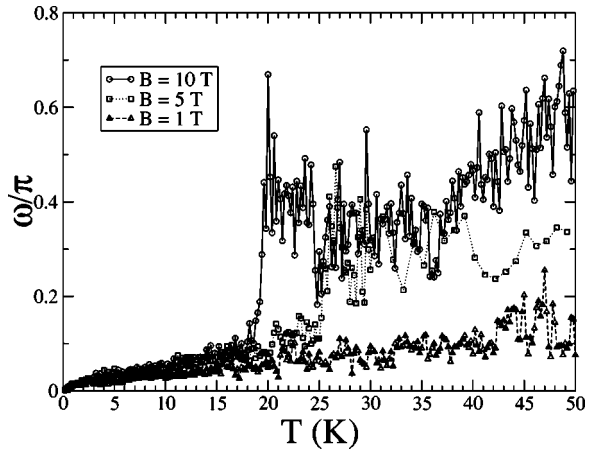

FIG. 7. T dependence of the average winding number of neighbor lines, usually associated with line entanglement. The discontinuity occurs at $T_m(B)$. Data using 10^5 MCS and $\Delta T = 0.2$ K.

Notice that the cage confinement, i.e., $\Delta r_{z,z_0} < a_0/2$, actually occurs in the solid phase at $T < T_m(B)$. In addition, contrarily to some recent theoretical suggestions,[15] the position $\mathbf{r}_i(z)$ of the decoupled pancake vortices, which once constituted a flux line in the solid phase, is such that $\Delta r_{z,z_0} \propto (zT)^{1/2}$, thus confirming Nelson's predictions[12] for the random-walk-like diffusion of melted lines, Eq. (1), and also in agreement with previous MC results.[19,20] However, in very low fields preliminary results do not exclude the occurrence of a disentangled or weakly entangled vortex liquid phase. It is also worth mentioning that the end-to-end rms displacement $\Delta r_{L_z,L_z/2}$ is usually associated with line entanglement. In this sense, for $B \geqslant 1$ T the entanglement criterion based on Eq. (3) is fulfilled at the melting temperature, as indicated by the arrow in the inset of Fig. 6(a) at $B = 10$ T: $\Delta r_{z,z_0} = a_0/2$.

Another measure of the line entanglement is commonly given by the winding number,[19]

$$\omega = \frac{1}{N} \sum_{ij} \left\langle \left| \sum_z \Theta(\mathbf{r}_i(z), \mathbf{r}_j(z)) \right| \right\rangle, \tag{20}$$

averaged over all nearest neighbor lines, which is plotted in Fig. 7. Here, Θ is the angle between $\mathbf{r}_{ij}(z)$ and $\mathbf{r}_{ij}(z-1)$. We notice that the discontinuity in ω is also present at $T_m(B)$ for $B > 1$ T, signaling that lines effectively begin to "entangle" at the melting transition.

Figure 8 displays the mean distance between two pancake vortices in the same *ab* plane which are neighbors in the solid phase:

$$\Delta r_{i,j} \equiv \sqrt{\langle [\mathbf{r}_i(z) - \mathbf{r}_j(z)]^2 \rangle}. \tag{21}$$

Below the melting temperature, $\Delta r_{i,j}$ hardly changes, although thermal defects start to proliferate in the vortex solid lattice. Even close to the melting transition, with the vortex lattice heavily distorted by these defects (as seen in Fig. 4), the mean distance between neighbor lines still remains little modified. In contrast, such a scenario changes dramatically above $T_m(B)$, where the large fluctuations in $\Delta r_{i,j}$ indicate a

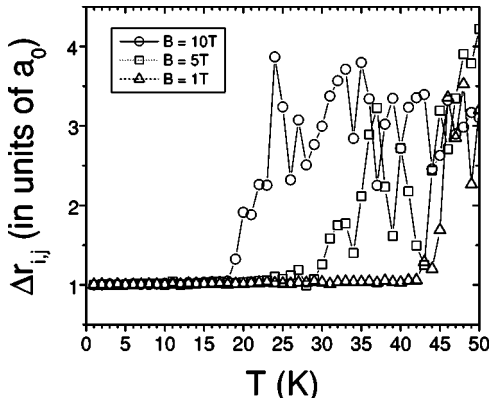

FIG. 8. T dependence at fixed B of the mean distance between two pancake vortices in the same ab plane which are neighbors in the solid phase, showing the considerable enhancement of their mobility in the liquid phase for $T > T_m(B)$. Data using 10^6 MCS and $\Delta T = 1$ K.

considerable enhancement of the vortex mobility in the liquid phase.

We have also measured the average number of collisions between pancakes, n_c. A collision between vortices occurs each time a bead (pancake vortex) makes a trial movement to a grid unit already occupied by another bead.[19] The results shown in Fig. 9 indicate that effects of cut and reconnection of lines become relevant only in $T > T_m(B)$ and are progressively incremented as the mobility of the pancake vortices enhances in the liquid phase, in agreement with results found using both the LD (Ref. 27) and the uniformly frustrated 3D XY (Ref. 19) models.

Finally, Figs. 10 and 11 display (H,T) diagrams of transition lines obtained with BSCCO samples in three distinct experimental works.[1,3,4] The nature of the transitions above the low-field first-order transition [$T_{FOT}(H)$ in Fig. 10; $H_{FOT}(T)$ in Fig. 11] is still controversial. Indeed, by measuring the flux penetration through a sample surface, Fuchs *et al.*[4] first associated T_x in Fig. 10 with a phase boundary characterized by the enhancement of the surface barrier. These authors also pointed out that the line along which the Bragg peaks disappear follows T_{FOT} at high temperatures and continues to follow the T_x line in higher fields.[44] In addition, based on a previous study using very low doses of columnar defects,[45] they mentioned that the vortex matter loses its shear modulus along the T_{FOT} line, rather than along the T_x line. From these considerations, the authors concluded that T_x is the melting line of a supersolid phase, although it remained to be determined which of the lines reflect thermodynamic phase transitions. On the other hand, Shibauchi *et al.*[3] extended these studies by using a sample-moving magnetization technique, from which they detected an anomaly in the magnetization curve, which was associated to T_x. By using Josephson plasma resonance to investigate the inter-

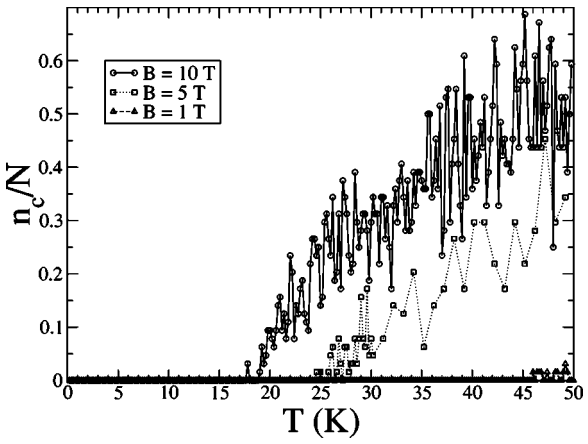

FIG. 9. T dependence of the average number of collisions between pancake vortices per line, associated with the emergence of cut and reconnection line processes. The onset above which n_c becomes finite coincides with $T_m(B)$. Data using 10^5 MCS and $\Delta T = 0.2$ K.

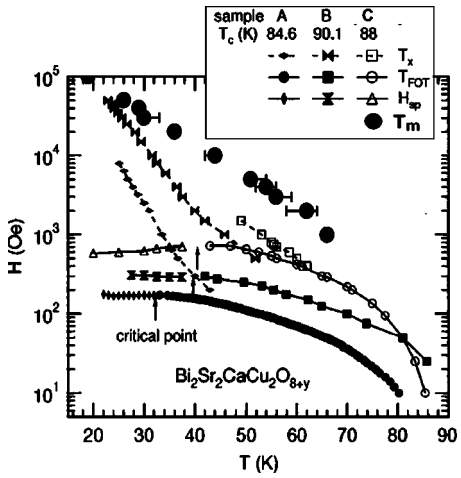

FIG. 10. Melting transition temperatures in high and intermediate fields using 10^5 MCS and $\Delta T = 1$ K (T_m, full circles), and phase diagram of BSCCO obtained by two independent experimental works, as in Ref. 3: samples A and B measured by Shibauchi *et al.*[3] sample C by Fuchs *et al.*[4] T_{FOT} is the low-field first-order transition temperature; H_{sp} marks the second peak in the magnetization curve; T_x is associated to the melting of a supersolid phase or to a surface-barrier related transition.

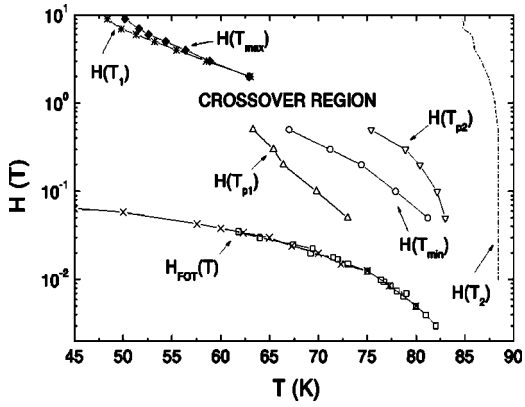

FIG. 11. Phase diagram of BSCCO as in Ref. 1: $H_{FOT}(T)$ is the low-field first-order transition; $H(T_{min})$ is a melting transition line; $H(T_{p2})$ is a decoupling line; $H(T_{max})$ is the line where $H(T_{p2})$ and $H(T_{p1})$ merge in high fields; $T_{p1}(H) < T < T_{p2}(H)$ is the interval where the "peak effect" is expected to occur.

layer phase coherence, these authors observed that, for fields above the T_{FOT} line, their measurements were consistent with the theoretical calculations[46] assuming the decoupled pancake liquid state. Further, at the T_x line they found no anomaly in the interlayer phase coherence. Therefore they concluded that the vortex decoupling does not occur at T_x, but, instead, T_x could be associated to the melting of a supersolid phase or to a surface-barrier related transition, although no clear-cut thermodynamic phase transition has been found. Finally, very recently, Torres *et al.*[1] measured the nonlocal in-plane resistance originated from transverse vortex-vortex correlations and associated $H(T_{min})$ to a theoretical 3D melting line[13,47,48] and $H(T_{p2})$ to the thermally induced 3D-2D vortex liquid decoupling transition in the vicinity of T_c (Ref. 49) (see Fig. 11). They also argue that the vortex pinning efficiency is enhanced in the interval $T_{p1}(H)<T<T_{p2}$ and that, for $H>0.5$ T, the lines $H(T_{p1})$ and $H(T_{p2})$ start to merge, whereas for $H>2$ T, a single transition in the vortex matter takes place at $H(T_{max})$, as seen in Fig. 11. From these studies, the authors concluded that a rigid vortex lattice exists for fields above the T_{FOT} line, over a wide region in the (H,T) phase diagram. In addition, in the intermediate field regime $(0.05\lesssim H\lesssim 0.5$ T) they found evidence for the vortex lattice melting and vortex liquid decoupling phase transitions, whereas in high fields ($H\gtrsim 2$ T) a vortex lattice melting-decoupling transition is supported by their measurements. These results[1,3,4] corroborate early studies[50] on the vortex lattice melting line in BSCCO.

Figure 10 also includes our MC data on $T_m(B)$, which suggests that the high-field line above T_{FOT} (Refs. 3 and 4) may indeed be associated with a strong melting-decoupling transition [$\xi_z\lesssim d$ above $T_m(B)$, for $B>1$ T, as seen in Fig. 5]. For intermediate fields ($0.1<B<1$ T), the vortex system exhibits a weaker first-order melting transition. These considerations (see also discussion related to results of Fig. 5) agree with the argument by Torres *et al.*,[1] which associated the high-field transition line to the merging of the 3D melting line and the 3D-2D vortex liquid decoupling transition. A better agreement between our MC results and the experimental ones is expected by using a suitable choice of parameters, although the low-field regime (in particular the T_{FOT} line) is outside the scope of our reported numerical simulations of a disorder-free system.

IV. CONCLUSIONS

We have performed extensive Monte Carlo simulations of clean strongly anisotropic BSCCO samples using the Lawrence-Doniach line model, which proved suitable to describe layered high-T_c superconducting oxides. In such strongly anisotropic compounds the nonuniformities of the magnetic induction become relevant, which makes the description through the 3D frustrated *XY* model less adequate. We have found first-order melting transitions in the intermediate and high-field regimes ($0.1\leqslant B\leqslant 10$ T), as indicated by the presence of discontinuity in the amplitude of the first Bragg peak of the planar density-density correlation function, the rms deviation of a pancake vortice, the rms deviation of the in-plane distance between pancake vortices, and in the hexatic order parameter. Contrary to early investigations by Ryu *et al.*[27] using the LD model, with smaller size systems and shorter MC running times, no clear indication of an hexatic phase was found, even in the single-layer limit. Discontinuities at the same melting temperature and field range have also been found in the winding number and the rms end-to-end line displacement, observables typically associated with line entanglement. In particular, in intermediate and high fields, our results on the end-to-end displacement have confirmed Nelson's predictions[12] for the random-walk-like diffusion of melted lines, as well as the cage confinement in the solid phase. In high fields, although previous results by Hellerqvist *et al.*[29] using the LD model suggest that decoupling of the superconducting CuO_2 layers occurs via a continuous crossover in this material, our results indicate a vortex lattice first-order melting-decoupling transition [$\xi_z\lesssim d$ above $T_m(B)$], corroborating early results on plane decoupling along the melting line found in *XY* model simulations[20,46] and elastic vortex theory,[43,49] and also in agreement with recent experimental observations in BSCCO.[1] Therefore we have found no entangled liquid phase in high fields.[7,12]

In conclusion, our results thus suggest that the LD model, as implemented in this work, may provide a quite reliable description of strongly anisotropic high-T_c superconducting materials. In fact, there are some similarities for the scenario in high magnetic fields using two different approaches, namely the *XY* and LD line models. Since they are based on distinct dominant mechanisms, these similarities require deeper physical interpretation. These results have stimulated us to pursue new applications of the method, under current investigation, in particular the behavior of the vortex matter in the presence of columnar disorder.[51]

ACKNOWLEDGMENTS

This work was supported by CNPq, FINEP, CAPES, and FACEPE (Brazilian Agencies). The authors are grateful to H. Brandt, G. Carneiro, M. Doria, E. Granato, Y. Kopelevich, and C. Olson for stimulating discussions. We also thank A. Batista and F. Moraes for collaboration in the very early stages of this work.

*Electronic address: lviana@lftc.ufpe.br
†Electronic address: ernesto@df.ufpe.br
‡Electronic address: mdcf@ufpe.br

[1] J. H. S. Torres, R. Ricardo da Silva, S. Moehlecke, and Y. Kopelevich, Solid State Commun. **125**, 11 (2003).
[2] N. Avraham, B. Khaykovich, Y. Myasoedov, M. Rappaport, H. Shtrikman, D. E. Feldman, T. Tamegai, P. H. Kes, M. Li, M. Konczykowski, K. van der Beek, and E. Zeldov, Nature

(London) **411**, 451 (2001).
[3] T. Shibauchi, T. Nakano, M. Sato, T. Kisu, N. Kameda, N. Okuda, S. Ooi, and T. Tamegai, Phys. Rev. Lett. **83**, 1010 (1999).
[4] D. T. Fuchs, E. Zeldov, T. Tamegai, S. Ooi, M. Rappaport, and H. Shtrikman, Phys. Rev. Lett. **80**, 4971 (1998).
[5] F. Bouquet, C. Marcenat, E. Steep, R. Calemczuc, W. K. Kwok, U. Welp, G. W. Crabtree, R. A. Fisher, N. E. Phillips, and A. Schilling, Nature (London) **411**, 448 (2001).
[6] See also comments about results of Refs. 2 and 5: P. Gammel, Nature (London) **411**, 434 (2001).
[7] C. J. Olson Reichhardt and M. B. Hastings, Phys. Rev. Lett. **92**, 157002 (2004), and references therein.
[8] G. P. Mikitik and E. H. Brandt, Phys. Rev. Lett. **89**, 259701 (2002); X. S. Ling, S. R. Park, B. A. McClain, S. M. Choi, D. C. Dender, and J. W. Lynn, *ibid.* **89**, 259702 (2002).
[9] X. S. Ling, S. R. Park, B. A. McClain, S. M. Choi, D. C. Dender, and J. W. Lynn, Phys. Rev. Lett. **86**, 712 (2001).
[10] E. M. Forgan, S. J. Levett, P. G. Kealey, R. Cubitt, C. D. Dewhurst, and D. Fort, Phys. Rev. Lett. **88**, 167003 (2002).
[11] S. R. Park, S. M. Choi, D. C. Dender, J. W. Lynn, and X. S. Ling, Phys. Rev. Lett. **91**, 167003 (2003).
[12] D. R. Nelson, Phys. Rev. Lett. **60**, 1973 (1988); D. R. Nelson and H. S. Seung, Phys. Rev. B **39**, 9153 (1989).
[13] G. Blatter, M. V. Feigel'man, V. B. Geshkenbein, A. I. Larkin, and V. M. Vinokur, Rev. Mod. Phys. **66**, 1125 (1994).
[14] J. Kierfeld and V. Vinokur, Phys. Rev. B **69**, 024501 (2004).
[15] A. M. Ettouhami, Phys. Rev. B **65**, 134504 (2002).
[16] A. K. Nguyen and A. Sudbø, Phys. Rev. B **60**, 15 307 (1999); **58**, 2802 (1998).
[17] E. H. Brandt, Phys. Rev. Lett. **63**, 1106 (1989).
[18] A. Houghton, R. A. Pelcovits, and A. Sudbø, Phys. Rev. B **40**, 6763 (1989).
[19] Y.-H. Li and S. Teitel, Phys. Rev. Lett. **66**, 3301 (1991); Phys. Rev. B **47**, 359 (1993).
[20] A. E. Koshelev, Phys. Rev. B **56**, 11 201 (1997).
[21] X. Hu, S. Miyashita, and M. Tachiki, Phys. Rev. B **58**, 3438 (1998); Phys. Rev. Lett. **79**, 3498 (1997).
[22] S. Ryu and D. Stroud, Phys. Rev. B **57**, 14 476 (1998).
[23] G. Carneiro, Phys. Rev. B **53**, 11 837 (1996); Phys. Rev. Lett. **75**, 521 (1995).
[24] R. Šášik and D. Stroud, Phys. Rev. Lett. **72**, 2462 (1994).
[25] J. Hu and A. H. MacDonald, Phys. Rev. B **56**, 2788 (1997).
[26] H. Nordborg and G. Blatter, Phys. Rev. Lett. **79**, 1925 (1997); Phys. Rev. B **58**, 14 556 (1998).
[27] S. Ryu, S. Doniach, G. Deutscher, and A. Kapitulnik, Phys. Rev. Lett. **68**, 710 (1992).
[28] A. K. Kienappel and M. A. Moore, Phys. Rev. B **60**, 6795 (1999).
[29] M. C. Hellerqvist, S. Ryu, L. W. Lombardo, and A. Kapitulnik, Physica C **230**, 170 (1994).
[30] S. Ryu and D. Stroud, Phys. Rev. B **54**, 1320 (1996).
[31] T. Klein, I. Joumard, S. Blanchard, J. Marcus, R. Cubitt, T. Giamarchi, and P. Le Doussal, Nature (London) **413**, 404 (2001), and references therein.
[32] D. R. Nelson, Physica C **263**, 12 (1996).
[33] D. R. Nelson and P. Le Doussal, Phys. Rev. B **42**, 10 113 (1990).
[34] L. P. Viana, E. P. Raposo, and M. D. Coutinho-Filho, Physica C **408-410**, 549 (2004).
[35] D. R. Nelson, *Defects and Geometry in Condensed Matter Physics* (Cambridge University Press, Cambridge, England 2002).
[36] G. W. Crabtree and D. R. Nelson, Phys. Today **50**(4), 38 (1997).
[37] $\xi_{z,c}$ in Eq. (2) is defined as one-fourth of the original one (Ref. 12) by the assumption that collisions are likely to occur whenever vortices wander half of the distance to their first neighbors ($\sim\sqrt{B/\phi_0}$).
[38] W. E. Lawrence and S. Doniach, in *Proceedings of LT 12, Kyoto, 1970*, edited by E. Kanda (Keigaku, Tokyo, 1971), p. 361.
[39] J. R. Clem, Phys. Rev. B **43**, 7837 (1991).
[40] G. Blatter, V. Geshkenbein, A. Larkin, and H. Nordborg, Phys. Rev. B **54**, 72 (1996).
[41] A. E. Koshelev, L. N. Bulaevskii, and M. P. Maley, Phys. Rev. B **62**, 14 403 (2000).
[42] M. C. Marchetti and D. R. Nelson, Phys. Rev. B **42**, 9938 (1990).
[43] M. V. Feigel'man, V. B. Geshkenbein, and A. I. Lakin, Physica C **167**, 177 (1990).
[44] E. M. Forgan, M. T. Wylie, S. Lloyd, S. L. Lee, and R. Cubitt, Czech. J. Phys. **46**, 1571 (1996).
[45] B. Khaykovich, M. Konczykowski, E. Zeldov, R. A. Doyle, D. Majer, P. H. Kes, and T. W. Li, Phys. Rev. B **56**, R517 (1997).
[46] A. E. Koshelev, Phys. Rev. Lett. **77**, 3901 (1996).
[47] E. H. Brandt, Rep. Prog. Phys. **58**, 1465 (1995).
[48] H. Safar, P. L. Gammel, D. A. Huse, S. N. Majumdar, L. F. Schneemeyer, D. J. Bishop, D. López, G. Nieva, and F. de la Cruz, Phys. Rev. Lett. **72**, 1272 (1994).
[49] L. I. Glazman and A. E. Koshelev, Phys. Rev. B **43**, 2835 (1991).
[50] A. Schilling, R. Jin, J. D. Guo, and H. R. Ott, Phys. Rev. Lett. **71**, 1899 (1993).
[51] L. P. Viana, E. P. Raposo, and M. D. Coutinho-Filho (unpublished).